

A SEMI-COLLOCATED OCEAN MODEL BASED ON THE SOMS APPROACH

DAVID E. DIETRICH

CAST, Mississippi State University, U.S.A.

AND

DONG-SHAN KO

RSMAS, University of Miami, U.S.A.

SUMMARY

In application to the Gulf of Mexico (GOM), a new DieCAST ocean model, which uses a modified Arakawa 'a' grid, and the SOMS model, which uses an Arakawa 'c' grid, give remarkably similar results. The new model avoids 'null space' problems of the standard 'a' grid approach by first using fourth-order interpolations to a 'c' grid advection velocity, then applying incompressibility to the result. Accuracy is further improved by using fourth-order pressure gradient approximations at 'a' grid locations. Incompressibility with general geometry is satisfied efficiently by a fast-converging iteration with a regular geometry elliptic solver. Results are compared with satellite-measured r.m.s. sea surface elevation anomaly and detailed front structures, climatological mean thermocline and empirical orthogonal functions and other observations.

KEY WORDS SOMS approach Ocean model

1. INTRODUCTION

The interaction between continental shelf and deep water flows typically occurs across a steep narrow shelfbreak. The need for better models of this interaction has spurred the development of the new DieCAST ocean model as part of the Semi-Enclosed And Coastal Ocean–Atmosphere Simulation Technology (SEACOAST) Project. The DieCAST model is a refined and extended version of the laterally 'semi-collocated' modified Arakawa 'a' grid approach described by Dietrich *et al.*¹ It evolved from the freestream submodel of the Sandia Ocean Modeling System (the SOMS model,^{2–4}), which uses an Arakawa 'c' staggered grid.

Z-level models such as the SOMS and Bryan–Cox^{5,6}, models are stable with large-amplitude steep topography when a surface pressure formulation is used.^{2,3,7} Thus a possible approach is to use a z-level model with lateral-boundary-fitted co-ordinates based on local depth contours. The 'a' grid is easier to use in boundary-fitted co-ordinates. However, it is not as widely used as the 'c' grid for incompressible flows. Here we show that an 'a' grid DieCAST model behaves quite like a 'c' grid model

We describe the DieCAST model in Section 2. In Section 3 we compare SOMS and DieCAST model results extensively with GOM observations and with each other. The SOMS model has also been applied with high lateral resolution (263 m) to Lake Neuchatel,⁸ the Gulf of Mexico^{9,10} and the vortex street in the wake of Barbados¹¹ and has demonstrated grid convergence in

resolution sensitivity experiments with a prototype ocean problem.¹ The DieCAST model is being applied to the Labrador Current (with Richard Greatbatch), the South China Sea (with Le Ngoc Ly), the Great Lakes (with Bill O'Connor), the Mediterranean Sea (with Paul Martin) and Hudson Bay (with Charles Lin). We plan to couple it to a sea-ice model.

2. DESCRIPTION OF THE NEW DIECAST MODEL

The DieCAST model is a hydrostatic, incompressible, rigid-lid, partially implicit, fully conservative ocean and lake model. The numerical differences from the SOMS model stem only from using an Arakawa 'a' grid instead of the Arakawa 'c' grid used by SOMS. The standard 'a' and 'c' grid approaches have well-known strengths and weaknesses. The 'a' grid is strong with the Coriolis terms but weak with the pressure gradient; the 'c' grid is weak with the Coriolis terms (however, see Reference 4) but strong with the pressure gradient. These two terms are the largest terms in the most energetic flow scales over most of the ocean. The approach taken by SOMS and DieCAST models is to use higher-order approximations and to interpolate between the 'a' and 'c' grids where appropriate to improve the weak terms. This leads to accurate and robust (stable with realistically small dissipation) models, which is important because the dominant ocean eddies are one to three orders of magnitude smaller than the world ocean, behave in a nearly inviscid manner and have not been successfully parametrized.

The SOMS model is described in detail in the references noted above. We briefly discuss the DieCAST model numerics here.

The DieCAST model solves all conservation equations on a common grid of cell-centred control volumes (the scalar cells in the SOMS model). The incompressibility (mass conservation) equation and pressure gradient terms, which are the weak points of collocated grids, receive special treatments as we now describe.

The first part of the special pressure gradient treatment is to use a special 'contravariant' horizontal advection velocity. This avoids the 'null space' pressure problems of the standard 'a' grid schemes. The contravariant velocity is defined by using fourth-order interpolations of the 'covariant' cell-centred results to the conventional staggered Arakawa 'c' grid locations. The incompressibility of the staggered advection velocity is then satisfied by 'clearing out' the divergence using a second-order hydrostatic elliptic pressure adjustment that is identical to the method used by SOMS and similar to the one described by Dukowicz and Malone.⁷ The resulting overall advection scheme is identical with the one used for the transport of scalar cell-centred quantities by SOMS. It is fully conservative, including quadratic energy-related quantities.

The second part of the special pressure gradient treatment is to use fourth-order approximations in the momentum equations at the 'a' grid locations. These use data spaced over four grid intervals on the collocated grid. For well-resolved flow components these approximations are more accurate than the standard second-order Arakawa 'c' grid approximations using data spaced over one grid interval.

Zones near boundaries require special evaluation of the pressure gradient. Fourth-order non-centred methods could be devised and investigated, but we use a simpler approach: we assign a zero value to the pressure gradient wherever boundary values are needed in its evaluation. These are substituted into our fourth-order scheme where needed near boundaries. (Our scheme is written as a combination of the four nearest pressure *differences* evaluated at 'c' grid locations.) The result is consistent with outflow points where the boundary tangential velocity and normal gradient of the normal velocity are given zero values. At rigid boundary points the geostrophic pressure gradient is zero, so this is consistent except very near the

boundaries. This simple approach thus seems reasonable for general circulation studies that do not resolve significantly non-geostrophic boundary regions. Comparison of 'a' grid DieCAST model and 'c' grid SOMS model results (see Section 3) shows that the boundary treatment has little effect, because the SOMS model uses the second-order standard 'c' grid approximation which never requires pressure values outside the water-containing zones.

The less accurate small-scale flow components are also robust with the DieCAST fourth-order pressure gradient. As with the SOMS model, the DieCAST model requires very little total dissipation for numerical stability. Although boundary points are less accurate, this can be compensated by a lateral-boundary-fitted version that is under development.

To avoid the need for elliptic rigid-lid pressure solvers applicable to island and irregular geometry, our models previously used a 'swamp layer' approach, beginning with Zuur and Dietrich.⁸ This involves artificially treating land locations as having one layer of highly viscous water such that it never accelerates significantly from rest. In practice, the initial flow at each time step is set to zero in top layer locations over land, which is equivalent to assuming an infinite bottom drag coefficient. Then the time step is carried out as if there were actually one layer of water over land. Except for a very brief initial transient during the first few time steps, this results in maximum velocities of water over land being greatly smaller than the velocities in the 'true' water regions and is thus a good approximation. We have demonstrated this by comparing the swamp layer approach with an exact approach in modelling flows around islands.^{11,12} The exact approach uses an efficient algorithm that iteratively applies a variable coefficient *regular* domain elliptic solver in such a way that convergence to exactly non-divergent flow with no flow over land is achieved (see Appendix).

The DieCAST model is simpler and runs slightly faster than the SOMS model. Its time step limit is determined mainly by a combination of internal waves and advection. Scaling gives internal wave speeds of roughly 3.5 m s^{-1} . Analytic determination would have to deal with highly non-linear stratification and our fourth-order pressure gradient. Maximum velocities are about 2 m s^{-1} , so a reasonable estimate for the fastest-propagating signal would be about 5 m s^{-1} . This gives about 30 min time step limit with 10 km resolution. We used a 20 min time step with $1/12^\circ$ (approximately 9 km) resolution ($192 \times 144 \times 20$ grid) in the Gulf of Mexico. This gives about 1700 days per CPU day on a single Cray YMP pipe (computing at an average rate of 210 M flops). The model fully vectorizes and parallelizes.

3. COMPARISON WITH THE SOMS MODEL AND GULF OF MEXICO OBSERVATIONS

The Gulf of Mexico (GOM) is dominated by its Loop Current, which feeds 25 million cubic metres per second into the Gulf Stream after passing through the Florida Strait. The Loop Current sheds major eddies that propagate westwards and dominate the western GOM circulation.

The SOMS and DieCAST models were recently applied to a series of GOM studies.^{9,10,13} Because of their low numerical dissipation, the models can realistically stimulate even small-scale features. This robustness with small-scale features is shown by Figure 1, which compares DieCAST-model-simulated small-scale Loop Current frontal structures with satellite observations dated 20 April 1984. The model simulation was *completely* determined by time-constant Caribbean Sea inflows, wind stress and surface fluxes (including both temperature and salinity effects). The surface fluxes are determined by restoring to specified surface conditions with a 30 day relaxation time. These were based *solely* on January climatological data which do not have these strong fronts. *No other data assimilation was used.* The temperatures are slightly cooler

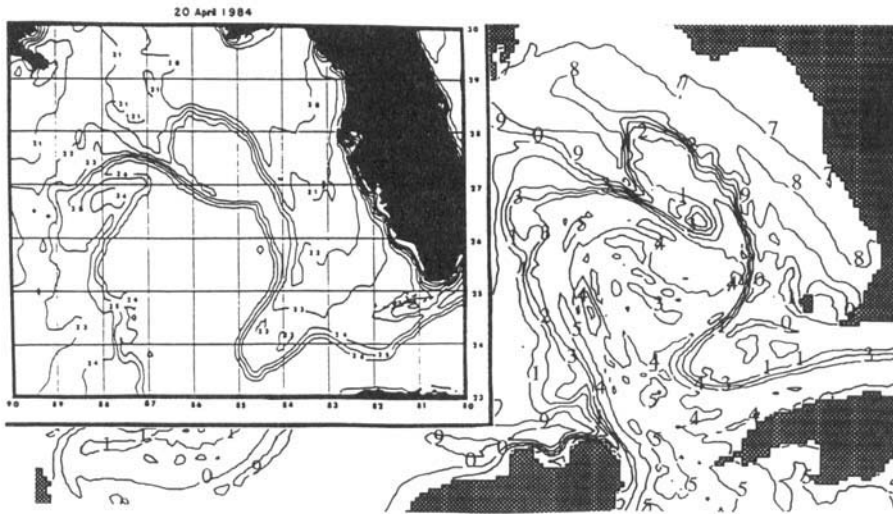


Figure 1. Top level (depth 10 m) temperature from the DieCAST Model and from observations (inset) in the Gulf of Mexico. The model snapshot is at day 1220 of a $1/12^\circ$ by 20 layer numerical simulation. The observations are sea surface temperature derived from a satellite image dated 20 April 1984 (p. 87, 'Gulf of Mexico Physical Oceanography Program Final Report, volume II', MMS publication 87-007, U.S. Department of Interior, Minerals Management Service, Gulf of Mexico OCS Region, New Orleans, LA, published by Evans Waddell and Murray L. Brown). The single-digit contour labels in the model output omit the 10's digit; thus e.g. the label '5' denotes a temperature of 25 °C

than they would be if April climatological restoring were used, especially in the longer-exposed water exiting the Florida Strait.

Case B3¹⁰ is probably one of the most extensively validated single runs ever in ocean modelling. Case B3 uses 20 layers vertical and 20 km horizontal resolution and is run for seven model years with prescribed time-independent inflow into the Caribbean patterned after observations.¹⁴ Open outflow conditions are prescribed in the Florida Strait. Local wind-forcing and thermohaline effects are ignored. Inflows are switched on full amplitude at the first time step. The results show shed eddy size (300 km), phase speed (4 cm s^{-1}) and mean shedding period (254 days) that are close to observations and theory. Figures 2–6 compare Case B3 results with observations.

Figure 2 compares with r.m.s. sea surface height anomaly derived from satellite altimetry. Major features are in close agreement.

Figures 3 and 4 compare with mean thermocline and empirical orthogonal functions derived from the full history of available GOM data. Only wintertime (January–March) data are included, because the wintertime surface mixed layer corresponds to the zero surface stratification resulting from the insulated surface condition used by the model. The model accurately simulates the mean thermocline. The model's deep water (minimum) temperature is 6 °C in both the initial conditions and the water entering the Caribbean rather than the 5 °C observed. The linear equation of state used in this study gives a bottom density at 6 °C equal to the 'true' non-linear value at 5 °C. The model's first empirical orthogonal mode contains most of the variance and is quite similar to observations (Figure 4). Its small vertical gradient near the surface reflects its insulated surface condition. The differences in the second and third modes are larger, but these contain relatively little of the variance. The remarkable agreement of the higher-order modes suggests that the observations are reliable even for such secondary modes.

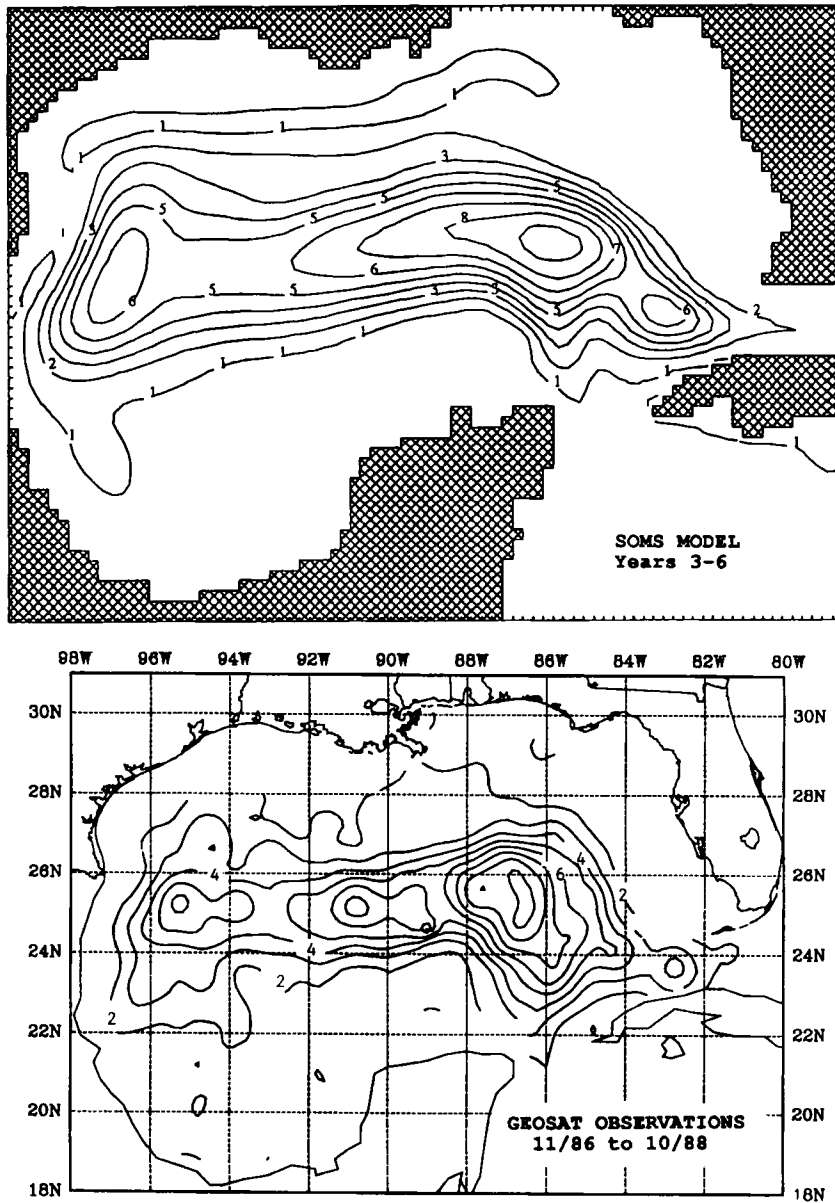


Figure 2. Comparison of model and observed r.m.s. sea surface height anomaly. Both plots have a 2.5 cm contour interval. To get the r.m.s. height in centimetres, multiply the single-digit contour labels by 2.5. The model equivalent sea surface height is derived

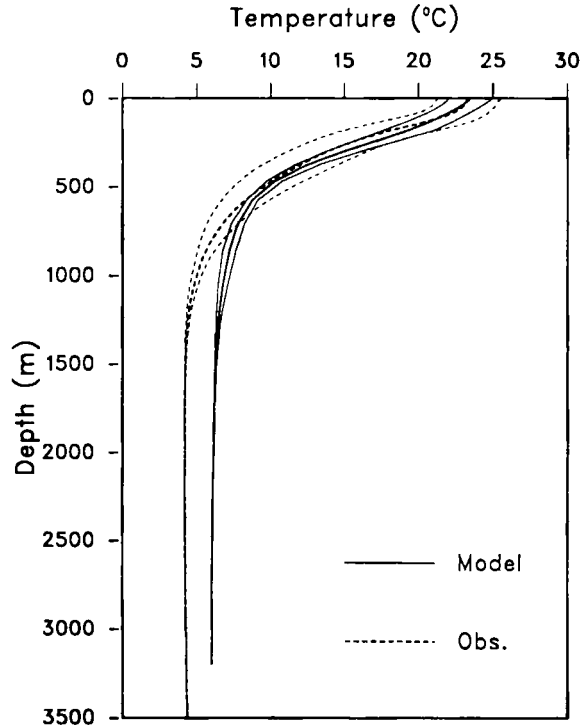


Figure 3. Comparison of model and observed vertical temperature profiles. These are laterally and time-averaged. Standard deviations are also shown

Figure 5 compares with the 'the most extensively studied eddy ever'.¹⁵ (More recently, even better data have been gathered for the Nelson Eddy.) The observations show a stratified surface layer typical of summertime conditions when they were made. The model emulates the mean climatological conditions which have a relatively deep surface mixed layer by assuming an insulated surface (no surface heat flux). The result is that, other than its surface mixed layer, the model is quite similar to the observations. Even secondary features are seen in the model results, including: a shallow cool pool near the centre of the Loop Current and recently shed eddies; and vertically coherent small-scale vertical displacements of the thermocline under the separated Yucatan western boundary current.

Figure 6 compares with observed counter-rotating eddies in the western GOM reported by Brooks and Kelly;¹⁶ Dietrich *et al.*¹⁰ show that the paired cyclonic eddies develop only when the lateral diffusivities are much smaller than $100 \text{ m}^2 \text{ s}^{-1}$ (Case B3 uses $20 \text{ m}^2 \text{ s}^{-1}$). The mechanisms of these and other features are discussed by Dietrich *et al.*¹⁰

Figure 7 compares SOMS and DieCAST model results for Case B3. The two models assimilate no data and use the same initial and boundary conditions, resolution and physical parameters. Thus the difference between the results is a measure of the truncation error difference between their grids. The first three major Loop Current eddy-shedding times agree within a few days in the two models (near days 570, 900 and 1210). Even secondary features are similar through the first three model years and nearly identical through the first eddy shedding cycle. The major eddy scale advection time scale is $O(10)$ days. Thus the remarkable similarity even after $O(1000)$ days supports the quality of both models as well as the extensive data used in their validation. It also suggests that if the boundary and initial condition errors are known with errors smaller than

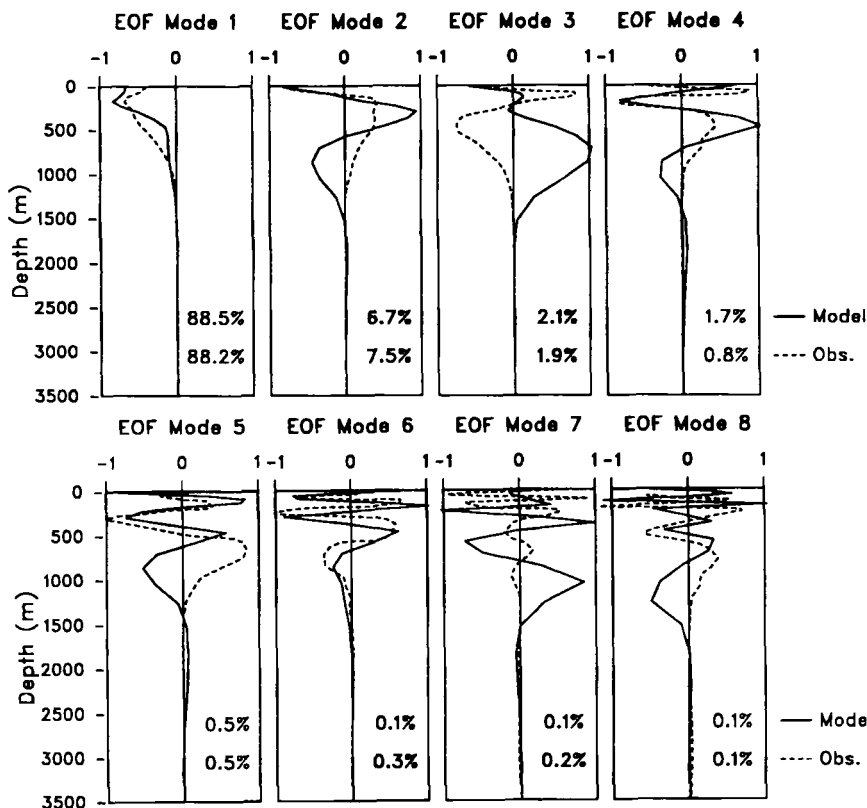


Figure 4. Comparison of model vertical empirical orthogonal functions with those from observations. The percentage of total variance represented by each EOF mode is given in each panel, with the observations value located above the model value

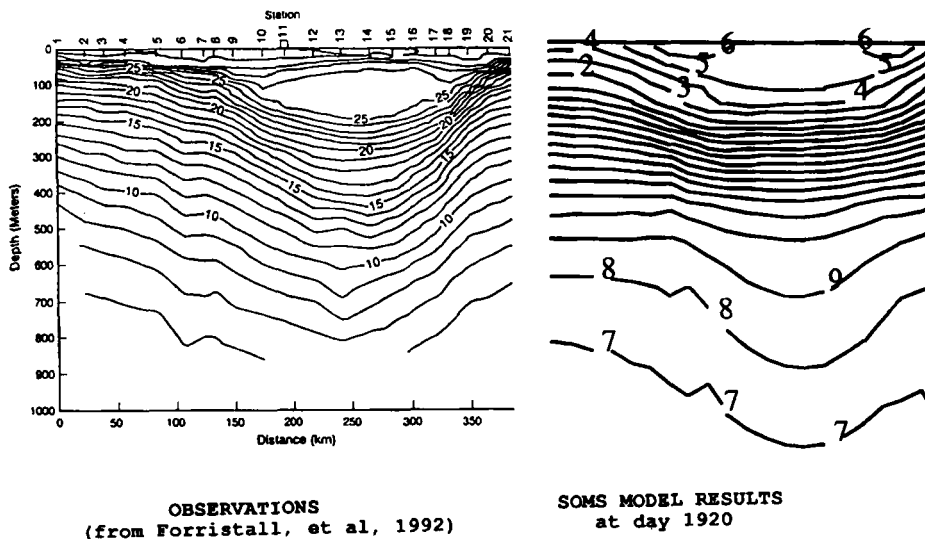
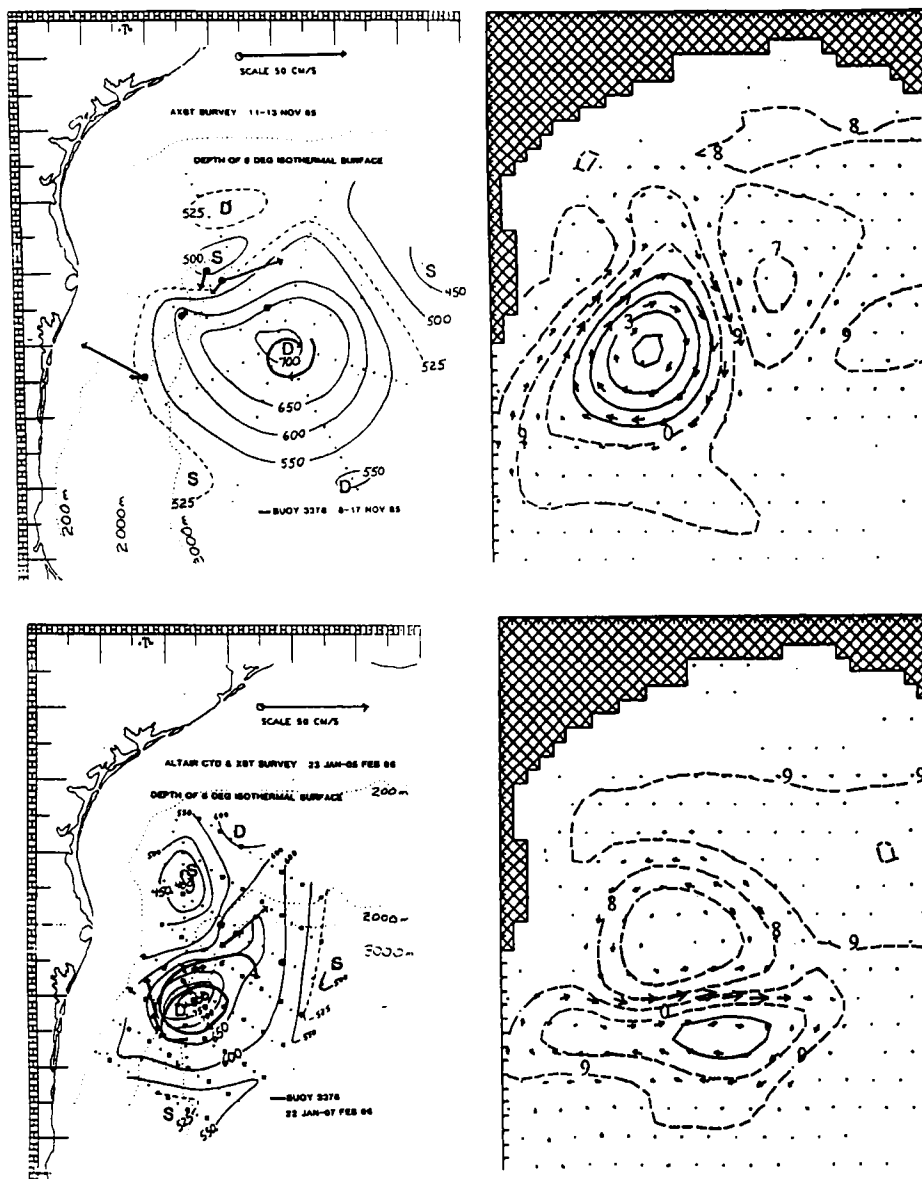
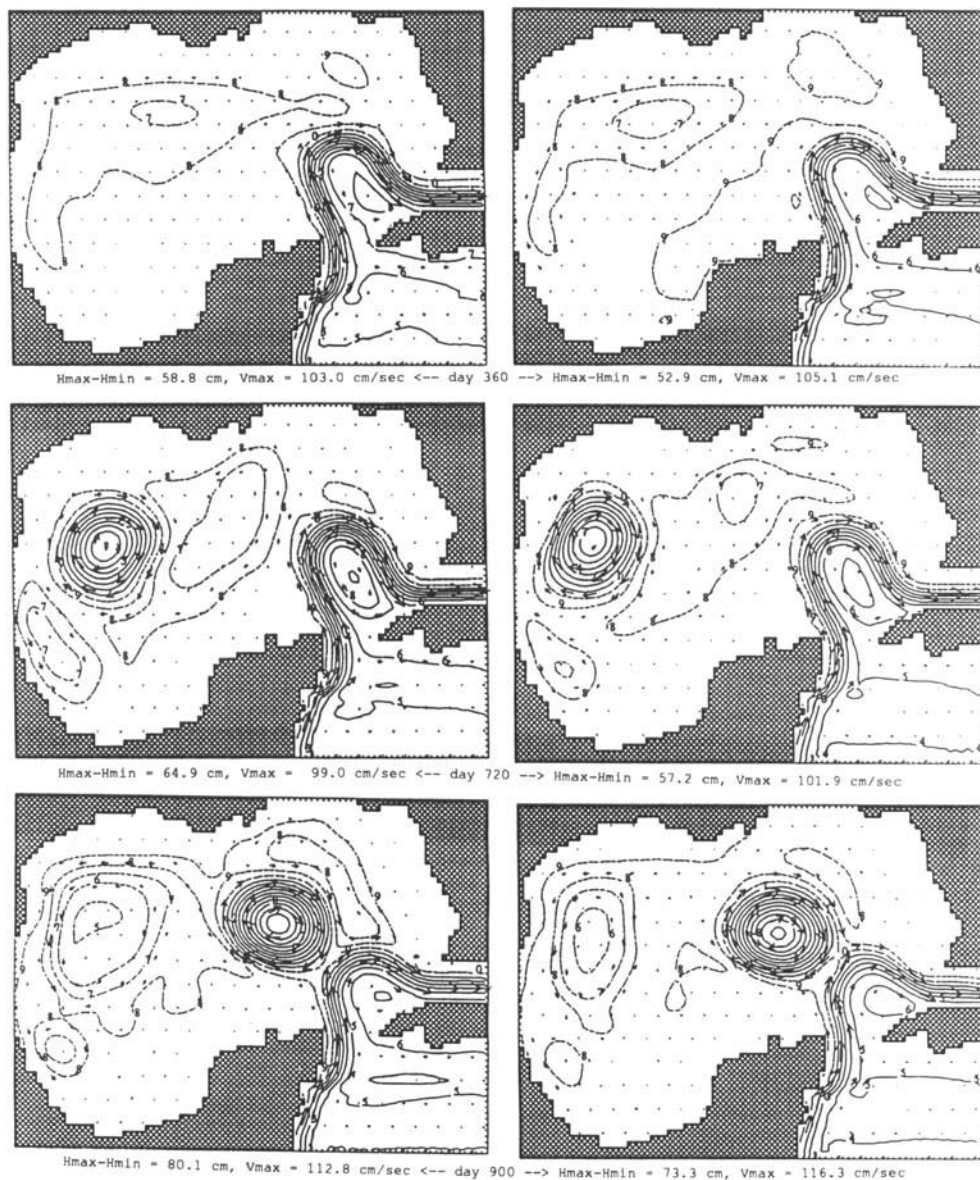


Figure 5. Vertical cross-sections of temperature ($^{\circ}\text{C}$) through a recently shed Loop Current eddy. The observations and model cross-sections have the same vertical and horizontal scales. The observations are from a NE-SW slice through the most thoroughly measured eddy ever. Model results are from a longitudinal-depth cross-section through the Loop Current core. The single-digit contour labels in the model output omit the 10's digit; thus e.g. the '6' isotherm near the top surface represents 26°C while the '7' isotherm near 900 m depth represents 7°C



OBSERVATIONS (Brooks and Kelly, 1986) MODEL RESULTS
 depth of 8°C isotherm top layer pressure and velocity

Figure 6. Paired eddy formation near the western GOM shelfbreak: observations and model results with no data assimilation. The observations are 80 days apart. The model results are 75 days apart (days 1935 and 2010 from Case B3). The maximum velocity in the region shown in the model results is about 50 cm s^{-1}



Arakawa "c" grid SOMS model

Arakawa "a" grid DieCast model

Figure 7. Intercomparison of two models in the Gulf of Mexico. Rigid-lid pressure (converted hydrostatically to free surface height anomaly) contours and velocity vectors are shown

the truncation errors of these runs, the GOM might be quite predictable through at least two eddy-shedding cycles.

In Figure 7 the DieCAST model gives realistically larger maximum Loop Current velocities (by a few per cent), while the total pressure range is slightly smaller than from the SOMS model. Apparently, the DieCAST model gives slightly more intense Loop Current fronts with the 20 km resolution used. Thus fronts, which contain a range of scales as in the Fourier series of a step

function, appear slightly better represented by the DieCAST model. The SOMS model could also be improved by using analogous fourth-order pressure gradient approximations, but the improvement would be limited by the accuracy of the Coriolis terms even with the fourth-order interpolations presently used.

4. CONCLUDING REMARKS

GOM observations include an extensive base of time-dependent aspects of GOM general circulation as well as detailed instantaneous snapshots. The close agreement of the SOMS ocean model with these observations even with steady inflow conditions and no transient data assimilation shows that *the natural time dependences that develop spontaneously with the SOMS model are very similar to the observed ones*. This supports the dynamic similarity of the SOMS model and the GOM. Such dynamic similarity is critical to reliable and useful application of ocean models.

The close agreement of $O(1000)$ day simulations in the GOM between the Arakawa 'c' staggered grid SOMS model and the new Arakawa 'a' semi-located grid of the new DieCAST model shows that truncation error has a secondary effect on major time dependences for at least $O(1000)$ days in both models. Thus *we have shown that two full primitive equation ocean models (SOMS and DieCAST) are dynamically similar to each other as well as to the real Gulf of Mexico* even though they use entirely different finite difference approximations because of their different grids.

The DieCAST model requires less computation per time step than the SOMS model when one takes advantage of metrics that are the same for all field variables. It is also stable with slightly longer time step, because the closest data used in the pressure gradient approximation are two grid intervals apart, which reduces the frequency of the smallest-scale-resolved internal waves compared with SOMS. (The time step increase depends on the ratio of the fastest flow velocity to the fastest internal wave speed.) Of course, the spatial accuracy of the smallest resolved scales is reduced compared with the Arakawa 'c' grid approach even with the higher-order approximations used.

ACKNOWLEDGEMENTS

We greatly appreciate useful suggestions by Harley Hurlburt, Dana Thompson, Steve Piacsek and Aaron Lai during the course of this research. This work was supported by the Office of Naval Research under Cooperative Agreement N00014-90-CA-001 with the University Corporation for Atmospheric Research.

APPENDIX: SURFACE PRESSURE SOLUTION IN IRREGULAR DOMAINS BY ITERATIVE APPLICATION OF A REGULAR DOMAIN ELLIPTIC SOLVER

Our basic surface pressure formulation is the same as used by Dietrich *et al.*² and Dietrich³ and similar to the one used by Dukowicz and Malone.⁷ However, we use a modified solution procedure algorithm that is better suited for vector and parallel computers when irregular boundaries and islands occur.

We start with a trial surface pressure such as from the previous time step. The hydrostatic relation is then applied to get the pressure everywhere below the surface. We then march the momentum equations one time step. We then determine a first surface pressure correction using Dietrich's aforementioned original procedure except that the top model layer is extended over land, resulting in a regular domain for the elliptic pressure solver. Thus, as part of an iteration to the exact solution, water is assumed to exist in a thin layer over land as well as in the 'true'

modelled ocean. The pressure correction is then applied to the flow. The flow over land is then set to zero. This results in non-zero divergence at 'true' water locations in the top level, but only along coastal boundaries. We then calculate a second pressure correction using Dietrich's procedure. When the new pressure correction is added to the first iteration result, the divergence is again exactly zero everywhere, but again there is some flow over land. However, it is greatly smaller than in the first iteration result. Further iterations can be carried out until the desired level of accuracy is achieved. In summary:

- (1) apply a regular geometry solver to get the first pressure correction
- (2) apply the pressure correction to get a non-divergent velocity
- (3) set the flow over land to zero
- (4) evaluate the residual (divergent velocity) error adjacent to the corrected land boundary points; if the residual is sufficiently small, the solution procedure is complete
- (5) solve for a pressure correction forced by the residuals and return to step (2).

Rapid convergence results because the residuals are highly localized along irregular coastal boundaries. This procedure greatly reduces the non-vectorizable and non-parallelizable computation often required by general direct elliptic solvers, while achieving much faster convergence than most iterative solvers. The direct solver used here is an EVP method^{17,18} which fully vectorizes or parallelizes in one of the two dimensions. This procedure is similar to the 'block implicit relaxation' methods used by Dietrich *et al.*¹⁹ for elliptic problems. Both are similar to domain decomposition methods and can be combined in application to large problems.

REFERENCES

1. D. E. Dietrich, P. J. Roache and M. G. Marietta, 'Convergence studies with the Sandia ocean modeling system', *Int. J. Numer. Methods Fluids*, **11**, 127-150 (1990).
2. D. E. Dietrich, M. G. Marietta and P. J. Roache, 'An ocean modeling system with turbulent boundary layers and topography: numerical description', *Int. J. Numer. Methods Fluids*, **7**, 833-855 (1987).
3. D. E. Dietrich, *The Sandia Ocean Modeling System Programmers Guide and Users Manual*, SAND92-7386, Sandia National Laboratories, Albuquerque, NM, 1992.
4. D. E. Dietrich, 'On modelling geophysical flows having low Rossby numbers', *Atmos./Ocean*, **31**, 57-71 (1993).
5. K. Bryan, 'A numerical method for the study of the circulation of the world ocean', *J. Comput. Phys.*, **4**, 347 (1969).
6. M. D. Cox, 'A primitive equation, 3-dimensional model of the ocean', *GFDL Ocean Group Tech. Rep. 1*, GFDL/NOAA, Princeton, NJ, 1984.
7. J. K. Dukowicz and R. C. Malone, *Parallel Ocean General Circulation Modeling*, LA-UR-92-200, Los Alamos National Laboratories, Los Alamos, NM, 1992.
8. E. A. H. Zuur and D. E. Dietrich, 'The SOMS model and its application to Lake Neuchatel', *Aquatic Sci.*, **52**, 115-129 (1990).
9. D. E. Dietrich and C. A. Lin, 'Numerical studies of eddy shedding in the Gulf of Mexico', *J. Geophys. Res.*, **99**, 7599-7615 (1994).
10. D. E. Dietrich, D.-S. Ko and L. A. Yeske, 'On the application and evaluation of the relocatable DieCAST ocean circulation model in coastal and semi-enclosed seas', *Tech. Rep. 93-1*, Center for Air Sea Technology, Mississippi State University, Stennis Space Center, MS, 1993.
11. M. J. Bowman, D. E. Dietrich and C. A. Lin, 'Observations and modeling of mesoscale ocean circulation near small isolated islands', in G. Maul (ed.), *Small Island Oceanography*, AGU, 1994.
12. D. E. Dietrich, M. L. Bowman and C. A. Lin, 'Numerical studies of small island wakes', in preparation.
13. D. E. Dietrich, 'Reynolds number and resolution sensitivity with western Gulf of Mexico eddies', in preparation.
14. W. J. Schmitz and P. L. Richardson, 'On the sources of the Florida Current', *Deep-Sea Res.*, **38**, S379-S409 (1991).
15. G. Z. Forrestall, K. J. Schaudt and C. K. Cooper, 'Evolution and kinematics of a Loop Current eddy in the Gulf of Mexico during 1985', *J. Geophys. Res.*, **97**, 2173-2184 (1992).
16. D. A. Brooks and F. J. Kelly, 'The interaction of a Loop Current ring with the continental shelf in the western Gulf of Mexico', *Proc. Seventh Ann. Gulf of Mexico Information Transfer-Meet.*, New Orleans, LA, November 1986, *OCS Study/MMS Rep. 87-0058*, 1987, pp. 255-300.
17. D. E. Dietrich, 'A program of elliptic solver development and implementation in semi-implicit numerical ocean models', *JAYCOR Final Rep. J510-81-053/2192*, 1981 (work sponsored by the Office of Naval Research, Naval Ocean Research and Development Activity).
18. P. J. Roache, 'Marching methods in elliptic equations', *Numer. Heat Transfer*, **1**, 1-201 (1978).
19. Dietrich *et al.* (1975).